Mechanism of nanodiamonds in the lapping of magnetic heads

Xionghua Jiang (494959636@qq.com)
Dongguan University of Technology

Research Article

Keywords: Nanodiamond, Mechanism of embedment, Hard disk head

Posted Date: May 3rd, 2021

DOI: https://doi.org/10.21203/rs.3.rs-355400/v1

Mechanism of nanodiamonds in the lapping of magnetic heads

Xionghua Jiang

School of Mechanical Engineering, Dongguan University of Technology, Dongguan 523000, P.R. China, Corresponding author

Corresponding author email:494959636@qq.com

Abstract

Nanodiamond, as the main component of slurry in the precision lapping process of magnetic heads, plays an important role on its surface quality. This paper studies the mechanism of nanodiamond embedded into Sn plate in the lapping process. The embedded pressure satisfies $p_0 = \frac{3}{2} \bullet \frac{W}{\pi a^2}$, and the embedded depth satisfies $\delta = k_1 \sqrt{P / HV}$. The above formulas are deduced from establishment of mathematical and physical models. AFM, SEM and AES are used to carry out surface quality detection and analysis of disk head. Results show that, both black spots on the surface and the removal rate have an important relationship with the nanodiamond. The experiments based on slurries with three different diameters（50 nm, 70 nm and 100 nm respectively）of nanodiamond are conducted, and the results show a better removal rate can be obtained with 100nm diamond embedded in the plate (21 nm • min^{-1}).

Keywords: Nanodiamond; Mechanism of embedment; Hard disk head

1. Introduction

Nanodiamond refers that diamond diameter under 100 nm. It not only has the

properties of diamond itself, but also has the special properties of nanoparticles, such as effects of small size, quantum size, surface, the macroscopic quantum tunnel [1-2]. In recent years, many scholars have done a lot of research on the stability, the continuity, and the shape, the particle size distribution, etc. of nanodiamond [3-4]. The nanodiamond aggregates easily, so the studies on dispersion of nanodiamond are particularly important, recent studies have focused on the thermodynamic stability of nanodiamond powder, dynamic stability and aggregate stability [5-8]. Many scholars have done many beneficial researches on the dispersion of nanodiamond in aqua system [9-12]. However, because of the metallic properties of magnetic head materials, lapping process requires non-aqueous system to avoid the possible existing of chemical corrosion. Dispersion of nanodiamond in nonaqueous systems directly affects the stability of its embedded in the plate, thus affecting the surface lapping quality of the magnetic head. Solid content and oil density and surface modifying agent of nanodiamond are considered to be the main factors affecting the dispersion of nanodiamond in nonaqueous systems [13-14]. Due to hard aggregation composed of Van Edward forces and hydrogen bonds, and soft aggregation caused by the surface atomic binding force, the methods to improve nanodiamond stability include: 1) Adding the surfactant to make the surface absorption or chemical reaction of the nanodiamond; 2) Using polymer nanodiamond powder instead of monomer, to avoid the particles getting too close; 3) Ultrasonic dispersion [15-17]. When using nanodiamond with good dispersion to preparing the slurry, it has high hardness, high heat transfer, high endurance and relatively better chemical stability [18-21]. When it

is used in the lapping of magnetic heads, the surface roughness can be greatly reduced [22-25]. Some scholars believe that the improvement mechanism is because of the existing ball bearing effect between the spherical nanodiamond and Sn plate, in which friction of rolling and gliding coexist. It can significantly increase lapping endurance and reduce the friction effect [26-27]. While some scholars believe that it is because of the existing boundary lubrication among the nanodiamond, the magnetic heads and the oil, which greatly reduces the friction [28]. There are few studies on the mechanism of nanodiamond embedded into Sn plate in the lapping process. In this paper, the mechanism of nanodiamond embedment is discussed by establishing the models, the two key factors, pressure of nanodiamond embedded into plate and the best value of embeded depth is studied, which have an important effect on the lapping surface of the magnetic head, especially the black spots and materials' removal rates of magnetic heads.

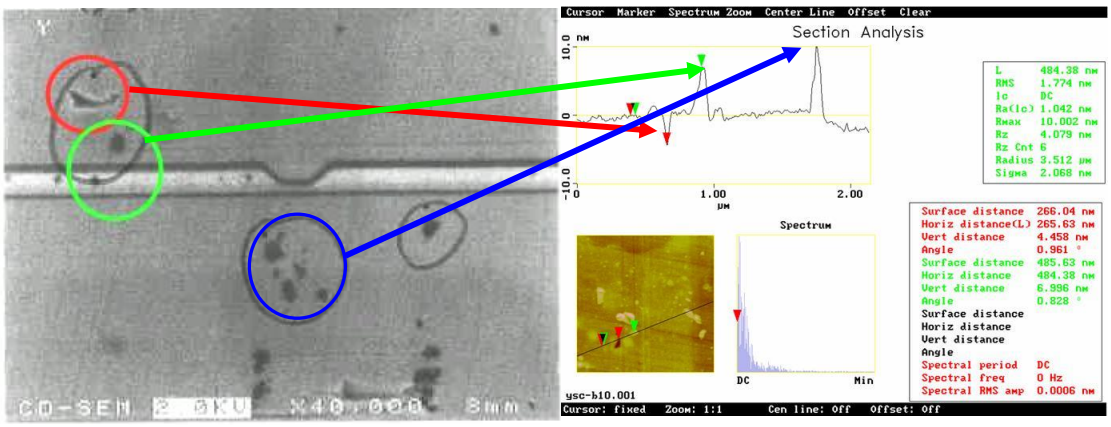

Fig.1 a) SEM pictures of black spots, Hitachi S4800 high resolution SEM, with Vacc 2.0 kV, × 40K. b) AFM pictures of the correspondent black spots on SEM pictures, PSIA AFM on tapping mode of PARK Company, Korea, and scan size is 10×40μm.

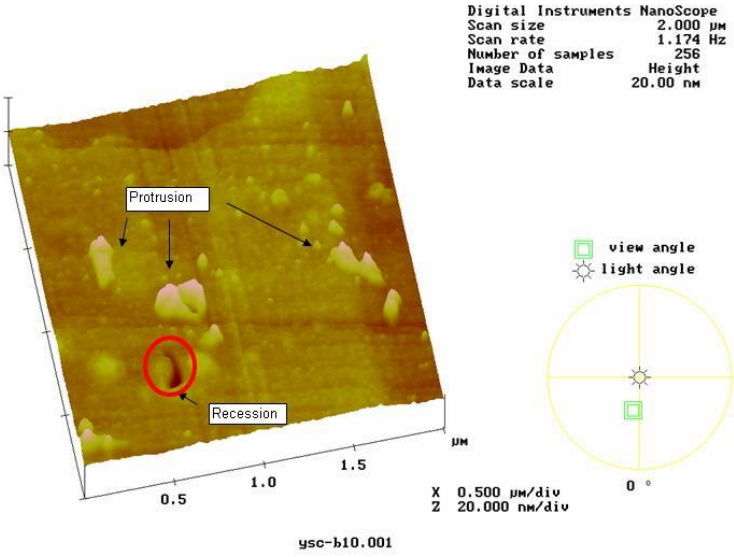

Fig.2 3D AFM pictures detected for protrusion (6.966nm) and recession（4.458nm） of black spots, PSIA AFM on tapping mode of PARK Company, Korea, scan size is 2μm.

As shown in Fig.1 and Fig.2, SEM and AFM pictures show the black spots on the surface of magnetic heads. Black spots refer to those spots usually bigger than 10nm in diameter, round with white reflection and the diamond-like protrusion. Since the capacity of holding nanodiamonds for Sn plate is limited, the pressure and embedded depth for nanodiamonds are very important.When the nanodiamonds are under less pressure, the embedded depth will be shallow, and the number of embedded particles will be less, which is hard for the materials of magnetic head to touch the diamonds in the lapping process. The nanodiamonds embedded into the plate surface are also easy to fall off and flow along with slurry. Both of the two cases will lead to low removal rate.

When the nanodiamonds are under bigger pressure, the embedded depth will be

deeper, the number of embedded particles will be more, resulting in the deformation of the Sn plate and more defects of the head surface including scratches, protrusion, recession, black holes, etc. AESE1127-08 is used to do further research on the composition of black spots, as shown in table 1. The experimental data confirmed that carbon content of the region with black spots is much higher than that of normal region. In this paper, the mechanism of embedded nanodiamond was discussed through the establishment of mathematical and physical models. The optimum value of the pressure and depth required for the nanodiamond embedment is studied deeply and using slurries with different diameters of nanodiamond to study their influences on removal rate of magnetic head materials.

Table 1 AES data for black spots

Composition	Black spots	Normal shield area
C	43.60%	18.90%
Ni	44.70%	64.10%
Fe	11.70%	16.90%

2 Establishment of model for nanodiamond embedment

2.1 Pressure analysis

Single diamond is considered first. Spherical diamond with 100nm diameter is used, while without moving or lubrication. The embedment accomplishes in two steps, as shown in Fig. 3.

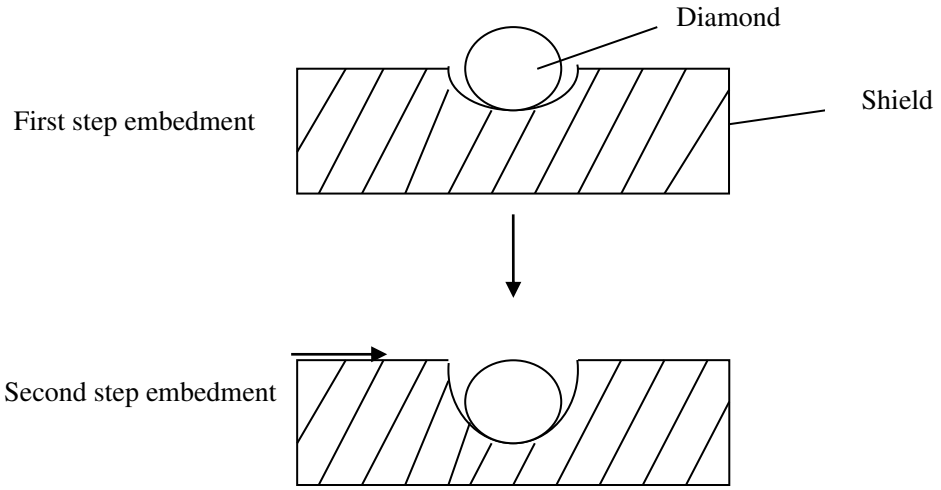

Fig. 3 Modeling of single diamond embedment

The mechanism of the process goes first from elastic deformation, next the elastic-plastic deformation, then turns to plastic deformation, and finally reached maximum plastic deformation. When a=r, the diamond is embedded into the shield.

Three values should be obtained: 1) maximum elastic deformation 2) maximum plastic deformation 3) corresponding pressure. In the first step, plastic deformation happens and the maximum deformation appears when half of the diamond is embedded into the shield. Based on classical plastic contact equation and considering adherent energy, we obtain:

$$P + 2\pi wr = \pi a^2 H \tag{2-1}$$

P refers to load, w, adherent energy, r, radii of diamond, a, radii of tough circle, H, hardness. ω can be obtained from (2-2)

$$w = 2\varphi(\gamma_a \gamma_b)^{1/2} \tag{2-2}$$

Where γ_a and γ_b refer to the surface force of shield and diamond respectively, and φ, related constant. When we regard r as the radius of circle in the case of maximum deformation，we get

$$P_1 = \pi r^2 H - 4\pi\varphi r(\gamma_a \gamma_b)^{1/2} \tag{2-3}$$

P_1, the pressure when plastic deformation begins.

In the second step, whole embedment happens. Based on classical contact mechanics theory,

$$a = \left(\frac{3WR_0}{E'}\right)^{\frac{1}{2}} - \left(\frac{3}{2} \bullet \frac{WR}{E'}\right)^{\frac{1}{2}} \tag{2-4}$$

$$\frac{1}{R} = \frac{1}{R_1} + \frac{1}{R_2} \tag{2-5}$$

$$\frac{1}{E'} = \frac{1}{2}\left(\frac{1-\nu_1^2}{E_1} + \frac{1-\nu_2^2}{E_2}\right) \tag{2-6}$$

Here, E_1=143 GPa, E_2=1141 GPa, ν_1=0.23, ν_2=0.07, thus E' =226.84 GPa. For spherical diamond, $R_2=R_0$, and $R_1=\infty$ for plane, thus $R=R_0$,

The largest pressure is $$p_0 = \frac{3}{2} \bullet \frac{W}{\pi a^2} \tag{2-7}$$

2.2 Indentation depth analysis

As shown in Fig.4, according to the test method of micro hardness, indentation depth δ is decided by hardness and load, as follows:

$$\delta^2 \propto P / HV \tag{2-8}$$

From the above formula, we have $\delta = k_1\sqrt{P/HV}$, where k_1 is a constant, related to the shape of diamond.

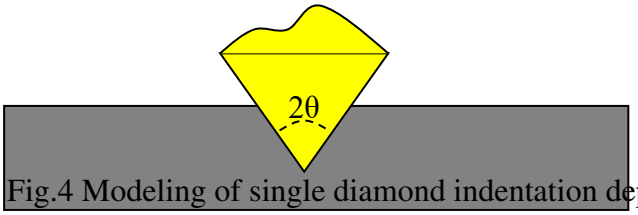

Fig.4 Modeling of single diamond indentation depth

3 Experiments

3.1 Material preparation

Three types of nanodiamonds extracted from CKK slurry with different radii, which were used for head lapping plate preparation, have been pictured by Hitachi S4800 high resolution SEM, with Vacc 5.0 kV (As shown in Fig.5).

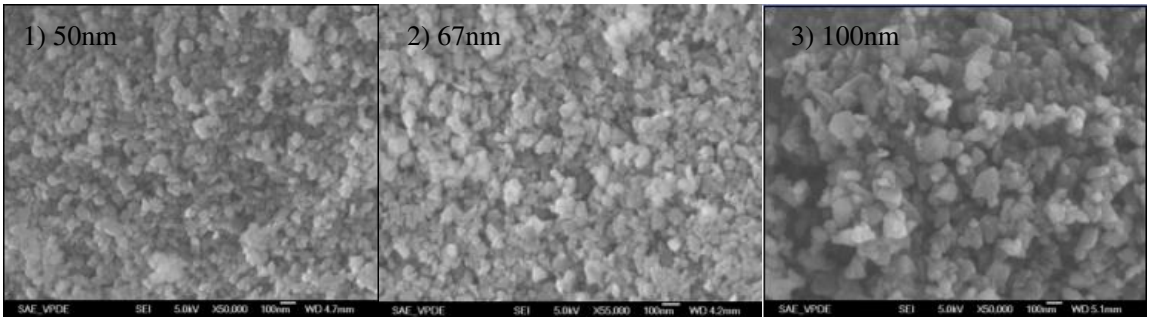

Fig.5 SEM pictures of diamonds 1) 50 nm diamonds from 1/20 CKK Co. USA. (×50 K) 2) 70 nm diamonds from 1/15 CKK Co. USA. (×50 K) 3) 100 nm diamond from 1/10 CKK Co. USA. (×50 K)

3.2 Machine and embedding process

Conditions: HYPREZ Lapping Machine from Engis Company, Japan was used. As shown in Fig.6，the Sn plate and the fixture were rotated by different motors through transmission belts to keep the lapping speed continually adjustable. Freeze water was used to ensure the constant of temperature by taking away the heat. The plate and the ring were rotated at fixed speed on the same direction. Rowbar was fixed on the ring with rubber, each rowbar (PMR, produced by TDK Co.) had 81 heads (sliders), and the size was 69.6×1.235×0.23 mm. Slurry was added by using capillary from bottle which stired constantly.

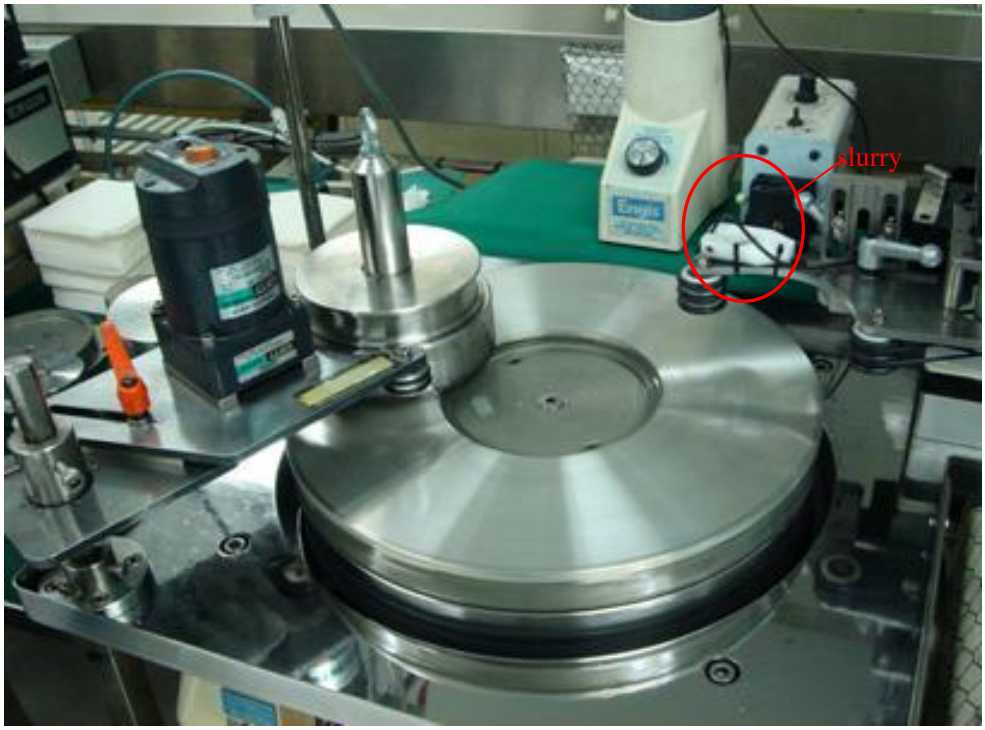

Fig.6 Lapping machine for nanodiamonds embedded into plate

The base material of the plate was Sn. The Rotation speed kept 30 rpm · min^{-1}. Ring rotation speed kept 25 rpm · min^{-1}, the weight was 6 kg and the shaving time was 25 mins. The lubrication was AM-ZX-60 from Engis Co. Removal rates were tested through calculating the resistant of magnetic heads before and after lapping by using SSCL-F precision magnetic test machine, which was made in TDK, Japan.

3.3 Results Discussion

3.3.1 Removal rates (shown in Table 2).

Removal rates are important for hard disk heads production, high removal rates are desirable, slurries with 50 nm and 75 nm nanodimonds have lower removal rate, 100 nm has normal removal rate.

Table 2 Removal rates comparison table by using nanodiamonds with different diameters

Diameter of nanodiamonds (nm)	Removal rate (nm/min)
1/20 CKK (50)	1.2
1/15 CKK (75)	6.966
1/10 CKK (100)	21

3.3.2 Removal rate calculation under plastic deformation

$$V = K_1 \bullet P \bullet H^{-1} \bullet L \tag{3-1}$$

Here, V--removal volume, P--pressure, H---hardness of removed materials, L---sliding distance, K_1--- a universal parameter decided by the friction coefficient, the shape of diamond, plate charging quality, toughness and plastic models of rowbar.

3.3.3 Removal rate calculation under crack deformation

$$V = K_2 \bullet P^{5/4} \bullet H^{-1/2} \bullet T^{-3/4} \bullet L \tag{3-2}$$

Here, P---pressue, H---hardness, T---crack toughness, L---sliding distance, K_2--- a universal parameter decided by the shape and radius of diamond. Both mechanisms take effect in the material removal. However, equation (3-1) and (3-2) show that the removal volume will increase if we raise the pressure (P) and sliding distance (L) is raised. Removal rate rises while weight increases. And when the plate speed is raised, L in unit lapping time increases, leading to the increase of removal rate.

4. Summary

The mechanism of nanodiamonds embedded into Sn plate has been discussed in this paper.

5. Acknowledgements

This work is supported by the lapping laboratory of SAE Technologies

(Dongguan) CO., LTD.

Declarations：

a. Funding (information that explains whether and by whom the research was supported)

The research leading to these results received funding from DGUT Ph.D. funding.

b. Conflicts of interest/Competing interests (include appropriate disclosures)

Not applicable

c. Availability of data and material (data transparency)

The authors confirm that the data supporting the findings of this study are available within the article. The raw data are available from the corresponding author upon a request.

d. Code availability (software application or custom code)

Not applicable

e. Ethics approval (include appropriate approvals or waivers)

Not applicable

f. Consent to participate (include appropriate statements)

Not applicable

g. Consent for publication (include appropriate statements)

Not applicable

h. Authors' contributions (optional: please review the submission guidelines from the journal whether statements are mandatory)

Not applicable

Reference:

[1] A.Gromov, S. A. Vorozhtsov, V. F. Komarov, G. V. Sakovich, Y. I. Pautova, M. Offermann, Mater. Lett. 91 (2013) 198.

[2] Eiji Osawa，Handbook of Advanced Ceramics (2nd Edition) (2013) 89.

[3] J. Mona, J.S. Tu, T.Y. Kang, C.Y. Tsai, E. Perevedentseva, C.L. Cheng, Diam. Rela. Mater. 24 (2012) 134.

[4] H.D. Wang, Q.Yang, H. Niu, I. Badea, Diam. Rela. Mater. 26 (2012) 1.

[5] E. Ōsawa, Diam. Rela. Mater. 16(2007) 2018.

[6] X.Z. Liu, T. Yu, Q.P. Wei, Z.M. Yu, X.Y. Xu, Coll. Surf. A: Phys. Engi.Aspe, 412 (2012) 82.

[7] Q. Zou, Y.G. Li, L.H. Zou, M.Z. Wang, Mater. Char. 60 (2009) 1257.

[8] I. Neitzel, V. Mochalin, I. Knoke, G.R. Palmese, Y. Gogotsi, Comp. Scie. Tech. 71 (2011) 710.

[9] Sumaiya，I. Raafat，N. Ibrahim, Tribol. Lett. 42 (2011)275

[10] G.M. Schmid, M.Miller, C. Brooks, J. Vacu. Scie. Tech. B: Micr. Nano. Stru. 27 (2009) 573.

[11] R. P. Ambekar, D.B. Bogy, Appl. Phys. Lett.92 (2008) 033104.

[12] S. H. Kim, Q. Dai, B. Marchon, J. Appl. Phys. 105 (2009) 07B704.

[13] S.Zhang, B.Strom, J. Trib.130 (2008) 011008.

[14] N.Liu, D.B. Bogy, Tribo. Lett. 33 (2009) 21.

[15] S.K Deoras, F.E Talke, J. Tribo.129 (2007) 177.

[16] N.Tagawa, A.Mori, K.Senoue, J.Tribo.129(2007)579.

[17] B.Tomcik, T.Osipowicz, J.Y.Lee, Thin. Solid. Films. 360 (2000) 173.

[18] K.Takata, J.Vacu. Scie. Tech. B: Micro. Nano.Stru. 27 (2009) 997.

[19] S. Weissner, Berkerly: Diss. Univ. Cali. 2001.

[20] S.J. Yoon, S.H. Son, D.H Choi, IEEE Trans. Magn.44 (2008) 151.

[21] T.R. Albrecht, F.Sai, IEEE Trans. Magn. 35 (1999) 857.

[22] M.A. Dufresne, A.K. Menon, IEEE Trans. Magn. 36 (2000) 2733.

[23] S.Yonemura, S.Weissner, L. Zhou, Tribo. Inte. 38 (2005) 81.

[24] Y.Hu, P.M.Jones, K. Li, J. Tribo.121 (1999) 553.

[25] S.Wang, F.P. Crimi, R.J. Blanco, Micro. Tech. 9 (2003) 266.

[26] J.P. Peng, J. Tribo.121 (1999) 568.

[27] J. Luo, D. Shu, B.Shi, Inte. J. Impa. Engi. 37 (2007) 1342.

[28] S.Kumar, D.Khanna, M. Sri-Jayantha, IEEE Trans. Magn. 30 (1994) 4155.

Figure Captions:

Fig.1 a) SEM pictures of black spots, Hitachi S4800 high resolution SEM, with Vacc 2.0 kV, × 40K. b) AFM pictures of the correspondent black spots on SEM pictures, PSIA AFM on tapping mode of PARK Company, Korea, and scan size is 10×40μm.

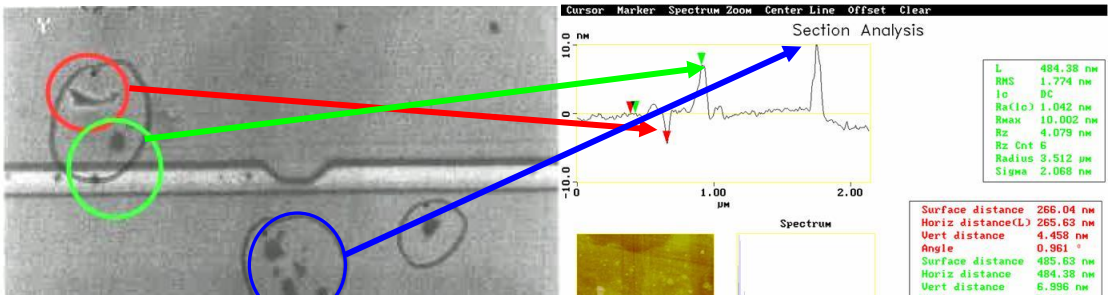

Fig.2 3D AFM pictures detected for protrusion (6.966nm) and recession（4.458nm） of black spots, PSIA AFM on tapping mode of PARK Company, Korea, scan size is 2μm.

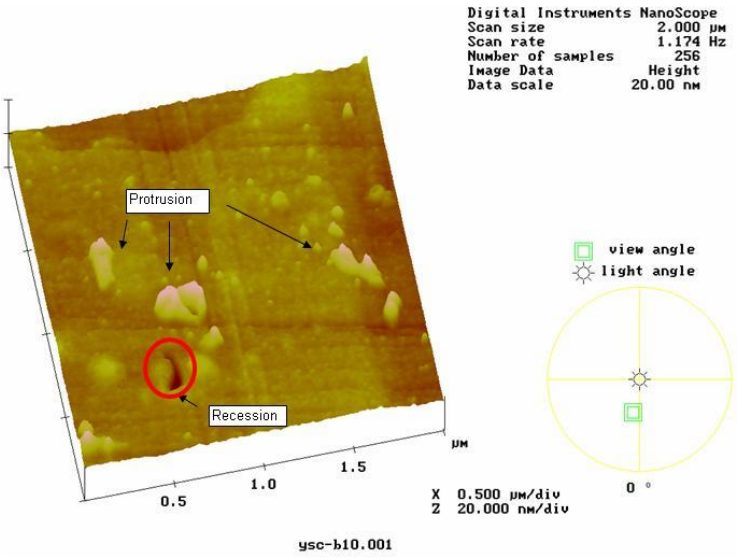

Fig. 3 Modeling of single diamond embedment

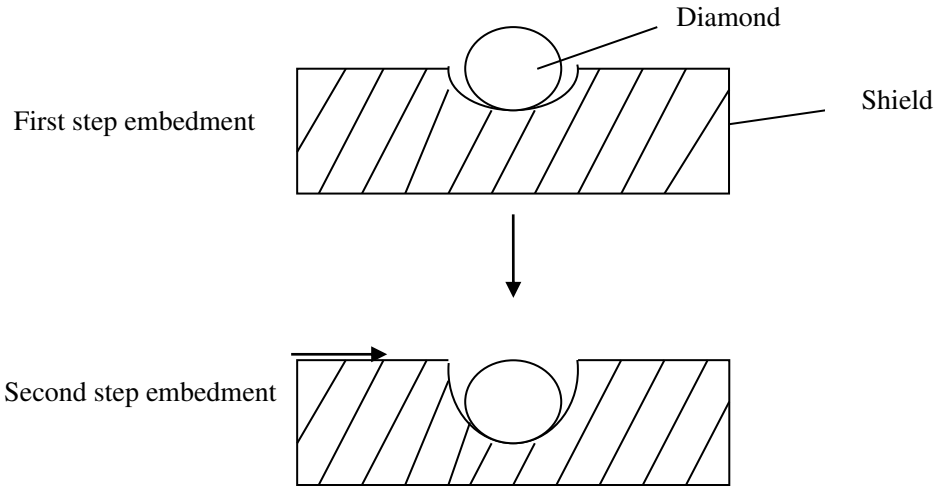

Fig.4 Modeling of single diamond indentation depth

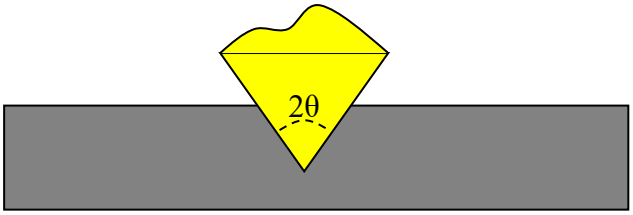

Fig.5 SEM pictures of diamonds 1) 50 nm diamonds from 1/20 CKK Co. USA. (×50 K) 2) 70 nm diamonds from 1/15 CKK Co. USA. (×50 K) 3) 100 nm diamond from 1/10 CKK Co. USA. (×50 K)

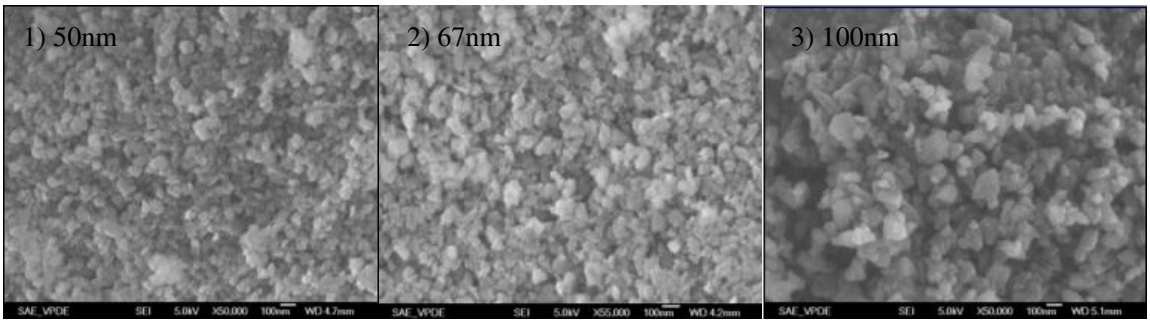

Fig.6 Lapping machine for nanodiamonds embedded into plate

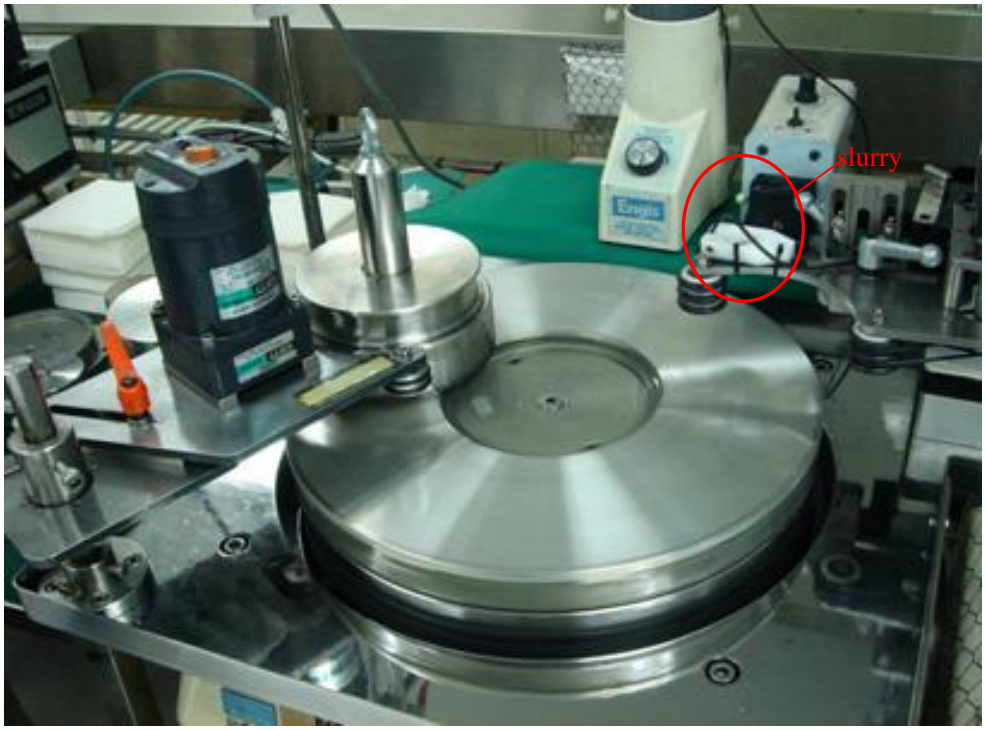

Table 1 AES data for black spots

Composition	Black spots	Normal shield area
C	43.60%	18.90%
Ni	44.70%	64.10%
Fe	11.70%	16.90%

Table 2 Removal rates comparison table by using nanodiamonds with different diameters

Diameter of nanodiamonds (nm)	Removal rate (nm/min)
1/20 CKK (50)	1.2
1/15 CKK (75)	6.966
1/10 CKK (100)	21

Figures

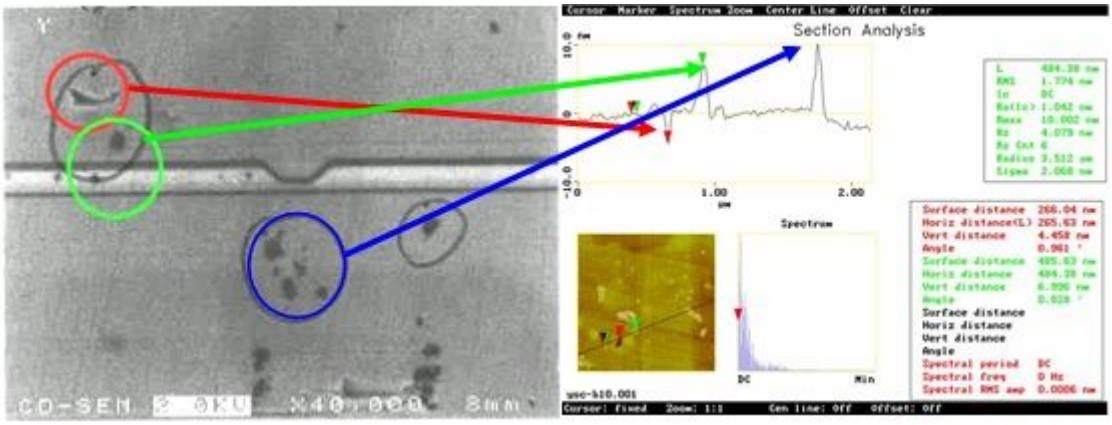

Figure 1

a) SEM pictures of black spots, Hitachi S4800 high resolution SEM, with Vacc 2.0 kV, × 40K. b) AFM pictures of the correspondent black spots on SEM pictures, PSIA AFM on tapping mode of PARK Company, Korea, and scan size is 10×40μm.

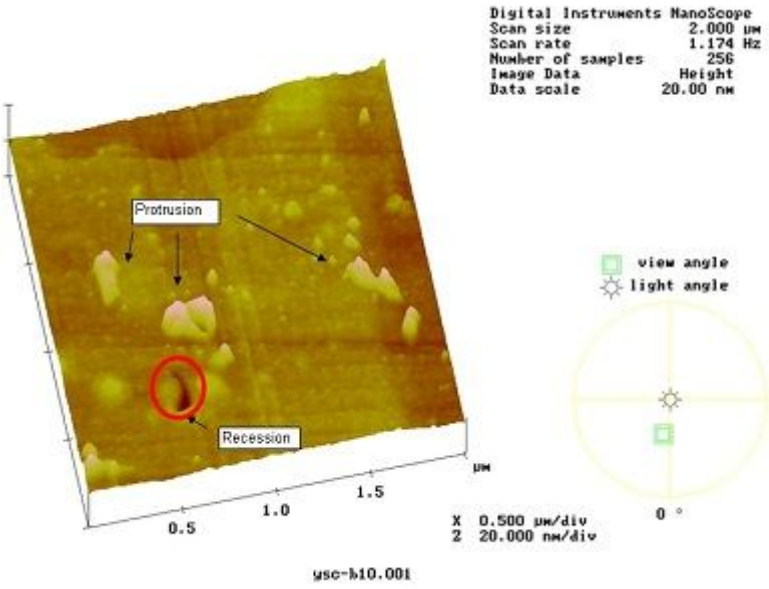

Figure 2

3D AFM pictures detected for protrusion (6.966nm) and recession（4.458nm）of black spots, PSIA AFM on tapping mode of PARK Company, Korea, scan size is 2μm.

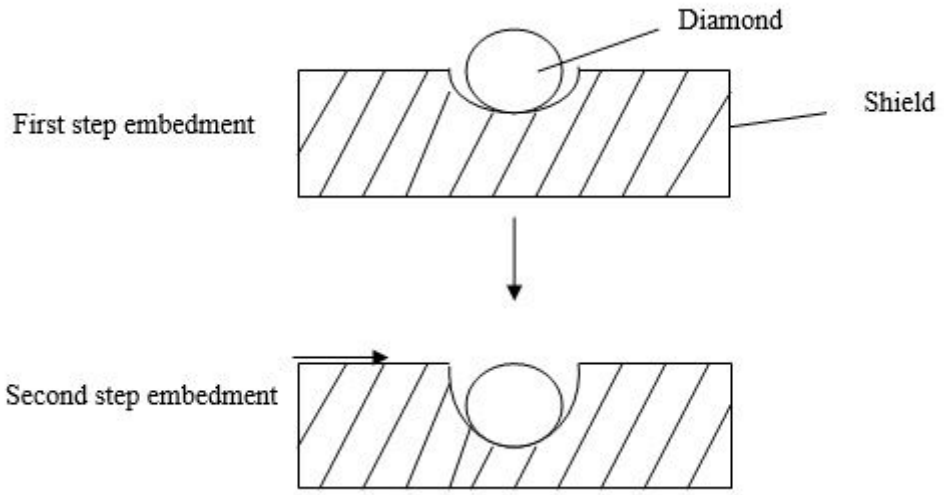

Figure 3

Modeling of single diamond embedment

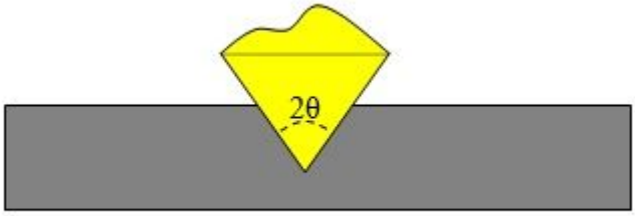

Figure 4

Modeling of single diamond indentation depth

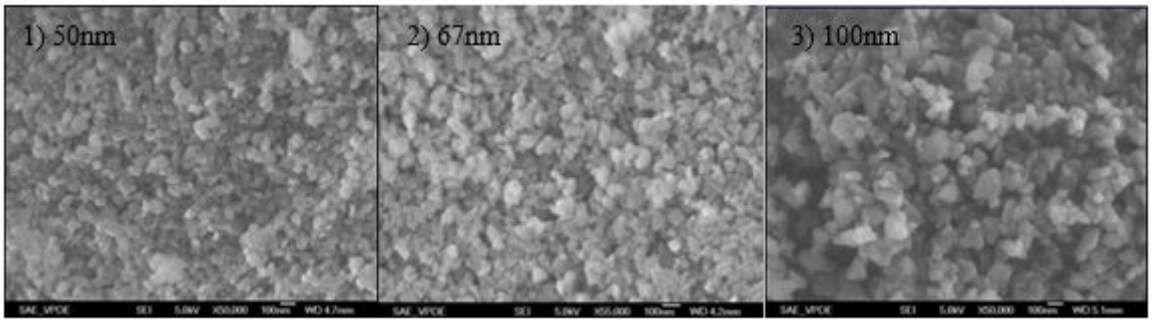

Figure 5

SEM pictures of diamonds 1) 50 nm diamonds from 1/20 CKK Co. USA. (×50 K) 2) 70 nm diamonds from 1/15 CKK Co. USA. (×50 K) 3) 100 nm diamond from 1/10 CKK Co. USA. (×50 K)

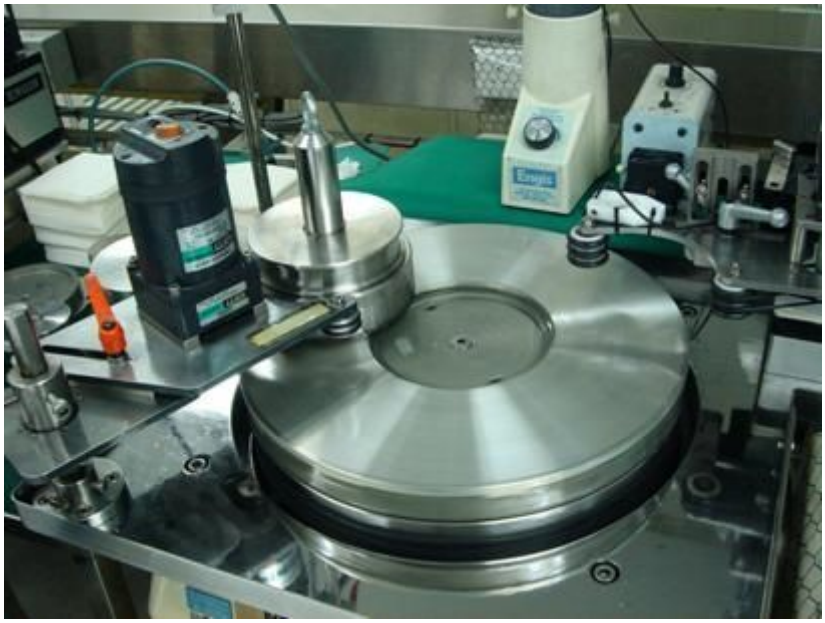

Figure 6

Lapping machine for nanodiamonds embedded into plate